CHAPTER 1

INTRODUCTION:

The increase in the complexity of the packing of electronic devices with highly integrated circuits (IC's) or electronic components generates electromagnetic (EM) interference (EMI) as by product[1,2]. EMI consists of EM noises which cause the reduction in the performance of the nearby electronic circuit/appliance or may pose human health hazards[3–5].EMI is a very common phenomenon that can be recognized even by a nontechnical person as radio static and distorted television reception in the form of flickers or flashes on the screen and click is sound or buzzing noise on audio systems ,arising due to external EM interferences[6]. EMI causes unnecessary loss of energy/resources, electronic malfunctioning or breakdowns, health hazards or even loss of precious human life.[6–8] Generally, high frequency signals are used in the operation of various electronic devices. Any transmittance of the EM fields created by these signals to surrounding environment may cause the malfunctioning of the nearby equipment. To prevent such EM hazards, our electronic devices should be shielded in such a way that both the incoming and outgoing interferences can get filtered out or suppressed. EMI shield is essentially a barrier to regulate the transmission of the EM wave across its bulk and in electronics terminology the, term 'Shield" usually refers to an enclosure which completely encloses an electronic product or a portion of that product and prevents the EM emission from an outside source to deteriorate its electronic performance.[1,9] All the electromagnetic waves (EM) consist of two essential components i.e. a magnetic field (H) and an electric field (E) as shown schematically in Fig 1. These two fields are perpendicular to each other as well as to the direction of the wave propagation.

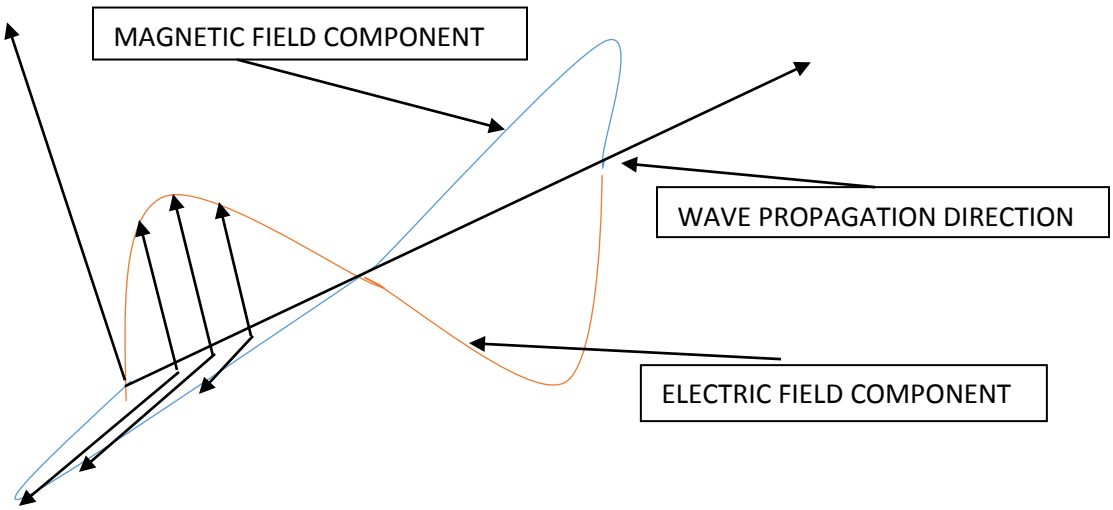

Fig.1 Schematic representation of EM wave and EM radiation vector

The performance of the shield is measured in terms of shielding effectiveness, which represents reduction in magnitude of incident power/field upon transition across the shield. which is shown in equation 1.

$$SE=20log_{10}\frac{E_t}{E_i}= 20log_{10}\frac{H_t}{H_i}. \text{ ---------- (1)}$$

Where E and H denote electric and magnetic fields respectively. Here, E is measured in the V/m and H is measured in the A/m, and the subscript t and i is referred to the transmitted wave and incident wave respectively.

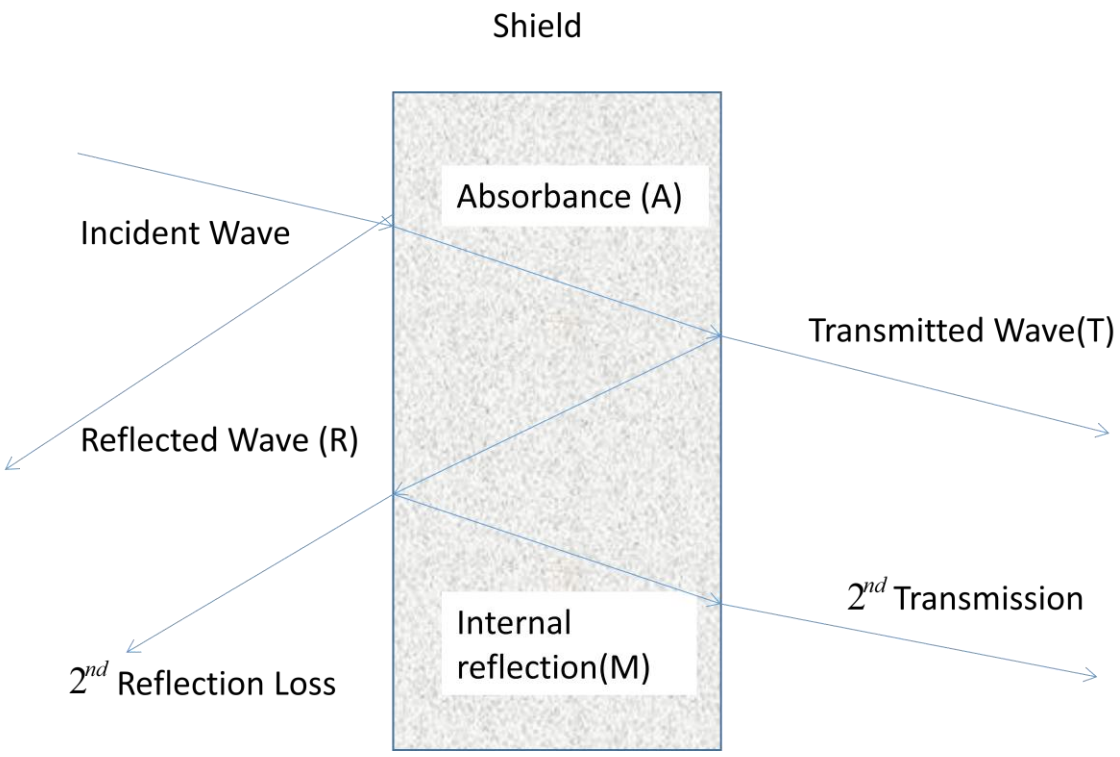

Fig.2 Schematic representation of EMI shielding mechanisms

In general, the three main shielding mechanisms (Fig. 2) viz. Reflection (R), Absorption (A)andmultiple internal reflections (M) contribute towards total shielding such that total shielding effectiveness (SE) in decibel unit (dB) can be expressed as 2:

$$SE\ (dB) = R\ (dB) + A\ (dB) + M\ (dB) \quad \text{---------- (2)}$$

The conventional materials like metals used in the EMI shielding are bulky, costly, corrosion prone and are highly reflective.[1,5,10] Because of the rigid and hardness nature of the metals, conducting polymer based blends and its Nano-composite shows some efficient results, but difficulties in their processing, and its stability remains an open challenge to implement in the market.[11–13]. The two main drawbacks of the conducting polymers composite i.e. difficult/poor

processibility and requirement of high filling levels, ultimately cause the deterioration of mechanical properties, electrical property and hence efficient shielding effects of materials. In this context, carbon based nanomaterials and their composites with advantages like light weight, metallic electrical conductivity, good mechanical properties, corrosion resistance, ease of synthesis and good process ability considered as an efficient choice for shielding materials and are widely used for the same.[1–3,5–7,10,14–22] The only disadvantages of carbon fibers and carbon nanotubes are that carbon fibers is very costly and carbon nanotubes is having high production cost, so the mass production of carbon nanotube based composite materials is very difficult. Recently, graphene, the atomically thin hexagonal lattice of carbon atoms, has gained enormous popularity due to its outstanding properties and wide range of proven applications. In this context, "graphene" has been envisaged as a promising EMI shielding material due to its ultra-high mechanical strength (Young's modulus ~1.0 TPa), tensile strength ~130 GPa, outstanding electrical conductivity (~10^6 S/m) and excellent thermal stability/conductivity[23]

In the recent past, various graphene analogues including graphene based foams,[24,25] nanocomposites,[26] aerogel,[27]graphene paper [28] have been explored for EMI shielding applications. Among them, graphene paper is considered as important EMI shielding material due to its good electrical properties, lightweight and flexibility. However, only few brief reports are available on the same and none of them explored the very high frequency shielding performance especially in the W band range (75–110 GHz) which is used for defense satellite communication, remote sensing or radar navigation.

In this thesis, we have tried to synthesis of graphene based thin paper and their measurement in high frequency EMI shielding. The graphene based paper is mainly prepared by three steps i.e. Synthesis of graphitic oxide (GO) by chemical oxidation,

Solution casting of aqueous dispersion of graphitic oxide to form sheet, and finally chemical reduction of dried GO paper to form reduced graphitic oxide (rGO) paper.

The formation of GO and its successful reduction to RGO phases is confirmed by optical images, FTIR & Raman Spectroscopy and XRD patterns. The EMI shielding performance of GOP and CRGOP is measured at 101 GHz frequency by free space technique and compared with attenuation of other flexible form of carbon i.e. expanded graphite (EG) sheet (EGS). We would like to emphasize that Shielding effectiveness studies of graphene analogues at such a high frequency have not been reported till date. The excellent shielding performance of CRGOP with total shielding effectiveness (SE) value of -35.49 dB (i.e. >99.97 % blocking of incident EM radiation) and specific SE value of -221.8 $dB.cm^3/g$ alongwith good flexibility, makes them potential candidate for lightweight EMI gasket material.

CHAPTER 2

LITERATURE SURVEY:

Conducting materials like conventional metals are very good conductors of electricity and it can absorb, reflect and Transmit electromagnetic signals/waves/ or interference. Whereas non conducting material or insulating material like rubbers and plastics are transparent to the EM signals or EMI. Because of good electrical conductivity and good thermal conductivity of the metals is the major advantages for their use in many applications. Heavy electrical equipments, in which the chances to build up of static charges is very high, are generally protected by grounding them with conductors generally metal so that the formed static charges and heat should be dissipated. In the same way, electromagnetic radiation which is having very high frequency should be either prevented from escaping from the equipment. So the equipment should be shield by metals or covers with the conducting materials. Materials which are used for the constructions of enclosures for shielding is conducting carbon materials like Polyaniline etc., a high permeability alloy of the composition of iron, copper, chromium, nickel with different ratio. Some other materials which are used as a shield are brass, aluminum, silver, nickel, stainless steel, metalized plastics and graphite composites. These composites are having some disadvantages like aluminum based has low impact resistance, where stainless steel are having high density. The metal shield are susceptible for corrosion. Because of the use of two different types of metals for shielding applications and gasket gives a result of galvanic corrosion because of which Leads to nonlinearity and decrease in SE of the metallic shields.[29,30]

2.1. SHIELDING MECHANISM

As already discussed earlier, three different Shielding mechanism contribute towards total shielding, whose detailed description is given below:

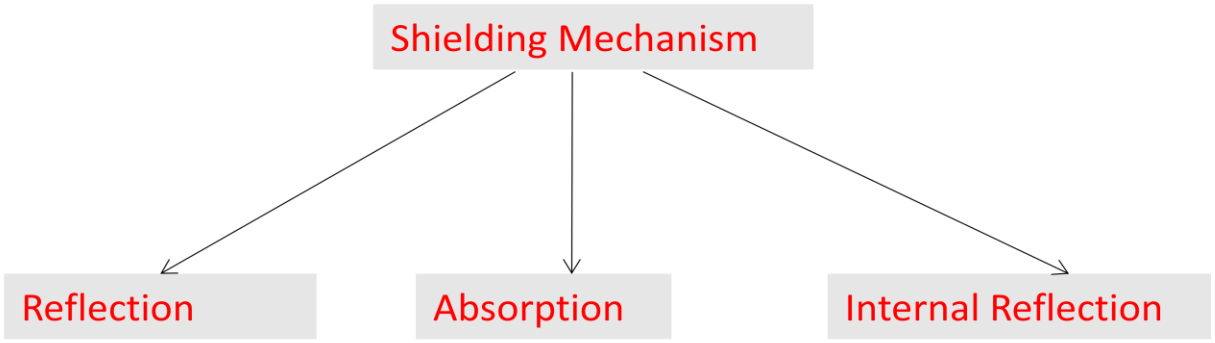

REFLECTION is the primary mechanism for shielding for which shield must have mobile charge carriers either electrons or holes, which interact with the EM field in the radiation so that the EM field get reflected. Its only due to the availability of free electrons in metals, they are the frequently used materials for EMI shielding and they function mainly by reflection. Because of bulkiness nature of metals, metal coatings can be done by electroplating, electroless plating or vacuum deposition are basically used for shielding purpose.[31–33]The coating should be given on bulk materials, fibers or particles, but Coatings tend to suffer from their poor wear or scratch resistance.

ABSORPTION is the secondary mechanism of EMI shielding. For better absorption of the radiation by the shield, the shield should contain electric and / or magnetic dipoles which will interact with the electromagnetic fields in the radiation. The electric dipoles will provided by the materials which is having a high value of the dielectric constant, and the magnetic dipoles will

provided by the materials which is having a high value of the magnetic permeability.[34]

The absorption loss of the EM wave is a function of the product$\sigma_r \mu_r$, and the reflection loss is a function of the ratio of $\frac{\sigma_r}{\mu_r}$, where σ_r is the electrical conductivity andμ_r is the relative magnetic permeability. Conventional Metals like Silver, copper, gold and aluminum are perfect for reflection mechanism, because of their high conductivity. Materials like Superpermalloy and mumetal are perfect for absorption, because of their high magnetic permeability. The reflection loss of the EM radiation will decrease with increase in frequency, while the absorption loss increases with increase in frequency.

Another class of shielding mechanism is MULTIPLE REFLECTIONS, which refers to the reflections at the various surfaces or interfaces in the shield. In the multiple reflection mechanism it requires the presence of a large interface area or surface area in the shield. An example of a shield with a large surface area is a porous or foam like material. The loss because of multiple reflections can be neglected when the distance between the reflecting surfaces or interfaces islarge compared to the skin depth.

Whatever is the losses, whether due to reflection, absorption or multiple reflections, they are commonly expressed in dB(decibel), and the sum of all the losses is called as the shielding effectiveness (in dB). The absorption loss is directly proportional to the thickness of the shield.

Penetration of EM radiation at high frequencies to the electrically conductor materials is defined as the skin effect. The electric field of a plane wave penetrating a conductor drops exponentially with increasing depth into the conductor. The depth at which the field drops to 1 /*e* of the incident value is called the skin depth (δ), which is given in equation 3.

$$\delta = \frac{1}{\sqrt{\mu\pi\sigma f}} \text{---------- (3)}$$

Where f is the frequency, μ is the magnetic permeability, σ is the electrical conductivity.

2.2. MATERIALS FOR SHIELDING

Due to skin effect, a composite material which is having small unit size of conductive filler is more effective than one which is having a conductive filler with a large unit size. Hence for effective and better use of the entire cross-section of a filler unit in the composite material for shielding, the unit size of the filler should be comparable to or less than the skin depth.

Polymer matrix composites which contains conductive fillers are very much attractive for shielding because of their processability (e.g. moldability), which helps us to reduce or to eliminate the seams in the housing which is the shield. The seams are commonly encountered in the case of metal sheets as the shield and they tend to cause leakage of the radiation and weaken the effectiveness of the shield. In addition, because of the low density of the polymer they are attractive for the composite preparation. The polymer matrix is mainly insulating in nature and does not help to shielding, however the polymer matrix can affect the connectivity of the conductive filler and hence connectivity will increase the shielding effectiveness. In addition, the polymer matrix affects the processability.[35,36]

Now a days electrically conducting polymers[37,38]are available, but because of their poor Processability and poor mechanical properties they are not so common in comparing to metal.

Electrically conducting polymer does not require any conductive filler to shield, hence they can be used with or without a filler. In the presence of a conductive filler, conducting polymer matrix has the advantage of being able to electrically connect the filler units that do not touch one another, and hence increase in the connectivity.

Cement is a little bit conducting matrix, so the use of a cement matrix with the conductive fillers allows the composite to be electrically connected, even when the filler units do not touch one another. Thus cement matrix composites have higher shielding effectiveness than corresponding polymer matrix. By using 1.5 vol% of discontinuous .1 mm diameter of carbon filaments can attain the shielding effectiveness of 40 dB at 1 GHz. Hence because of less expensive of cement than that of polymers, cement matrix composites are very useful for the shielding of rooms in a building [34,39]. In comparison with carbon it is a superior matrix than that of polymers for shielding due to its good conductivity, but carbon matrix suffers with high cost .

A seam which is mainly use in a housing which serves as an EMI shield should need to be filled with an EMI gasket, gasket is a very good EMI shielding material, which is based on a material like elastomer, such as rubber[40]. An elastomer is also a strong material, but itself is not able to shield the EM radiation, unless it is coated with any conductor (e.g. a metal coating called metallization) or is incorporated with a conductive filler mainly a metal fillers. The coating will suffer from its poor wear resistance and the use of a conductive filler will suffer from the resulting decrease in flexibility, especially with a high filler volume fraction that is usually required for sufficient shielding effectiveness. As the decrease in flexibility becomes more severe as the filler concentration increases, so the use of a filler that should be very effective even at a low volume fraction should be desirable[41,42]. Hence, the development of EMI gaskets is

more challenging in the present scenario than that of EMI shielding materials in general.

Synthesis of a general EMI shielding material in the composite form of material, a filler whichshould be effective at a low concentration is also desirable, while it is not as critical as for EMI gaskets. This is because of the increase in filler content filler matrix bonding is poor and hence the ductibility and the strength will tend to decrease. Poor bonding is very common in thermoplastic polymer matrices. Moreover, a low filler content is also desirable due to its better Processability, which will decreases with increase in viscosity. In addition, a low filler content is desirable due to the cost saving and weight saving.

In order for a conductive filler to be highly effective, it should have a small unit size comparative to the skin depth, a high conductivity for shielding by reflection mechanism and a high aspect ratio for connectivity in the matrix, hence Fibers are more attractive than particles because of their high aspect ratio.

Carbon fibers is more use in EMI shielding applications[43,44].Becasue of the small diameter, carbon filaments are more effective at the same volume fraction in a composite than that of the conventional short carbon fibers for EMI shielding applications, as shown for both thermoplast[37,40] and cement[34,37] matrices.

For example, in below table 1 it can be clearly shown that how SE depends on the filler percentage of the carbon fillers.

Matrix	Volume % of carbon fillers	SE in dB	Frequency in GHz	Volume% of carbon fillers	SE in dB	Frequency in GHz
THERMOPLAST	19	74	1	20	46	1
CEMENT	.54	26	1.5	.84	15	1.5

Table 1. Matrices with different vol. % and their shielding effectiveness.

In the thermoplast matrix, carbon filaments with 19 vol.% gives an EMI shielding effectiveness of 74 dB at 1 GHz,whereas carbon fibers at 20 vol.% give a shielding effectiveness of 46 dB at 1 GHz. In the cement matrix composite, the volume fractions of fiber typically less than 1%. Carbon filaments at 0.54 vol. % in a cement paste give an effective-ness of 26 dB at 1.5 GHz , whereas carbon fibers at 0.84 vol. % in a mortar give an effectiveness of 15 dB at 1.5 GHz[21]. These shielding effectiveness measurements were made with the same fixture and about the same sample thickness.

Conventional metals because of their high conductivity are more attractive towards shielding than that of carbons, though carbons are more attractive in their oxidation resistance and thermal stability. So, metal fibers of small diameter in size are most desirable, though metal fibers which is made by forming or casting cannot be finer than about 2 mm. but, metal fibers with submicron diameter can be formed by coating submicron diameter carbon filaments with a metal. For example Ni filaments with diameter 0.4 mm, can be made by electroplating of 0.1 mm-diameter carbon filaments with Ni, have been shown to be particularly effective[45]. They are known as Ni filaments because they mostly contain Ni rather than the carbon. With only 7% of volume of Ni filament a shielding effectiveness of 87 dB at 1 GHz can be attained in a polymer matrix composite. Nickel is more attractive metal than that of copper, because of its superior oxidation resistance. The oxide film is poor in conductivity and is thus poor in connectivity among filler units.

Table 2 compares the EMI shielding effectiveness of polyethersulfone matrix composite[21,46] with various fillers at 1–2 GHz of frequency and the sample thickness of 2.8 mm. The shielding effectiveness for all specimens was determined by the coaxial cable method using the same tester. Even at a low filler content of 7 vol.%, the nickel filaments provide much greater

shielding effectiveness than all the other fillers of Table 2.

In comparison to PES, nickel particles of size 1–5 mm gives better EMI shielding effectiveness at 1–2 GHz than that of silver particles of size 0.8–1.35 mm. Together with Table 2, this means that nickel filaments provide better shielding effectiveness than that of silver particles.

FILLER	VOL %	SE in dB
Aluminium flakes	20	26
Steel fibers	20	42
Carbon fibers	20	19
Ni particles	9.4	23
Ni fibers	19	5
Ni fibers	7	58
Carbon filaments	7	32
Ni filaments	7	87

Table 2.EMI shielding effectiveness at 1-2 GHz of PES matrix composites with various fillers

The submicron diameter filaments which are mentioned above are discontinuous and hence arenot sufficient for providing structural composites, which restricts it in the application of aircraft and electronic enclosures. Thus Continuous fiber of polymer matrix structural composites that are capable of EMI shielding and are needed for aircraft and electronic enclosures[46]. The fibers used in these composites are mainly carbon fibers (of diameter around 10 mm), which may be coated with a metal (e.g. nickel[45]) or doped to increase the conductivity.

2.3. FLEXIBLE GRAPHITE FOR SHIELDING

An attractive EMI gasket material is made up of graphite which should be flexible in nature, and the flexible sheet formed by compressing a collection of exfoliated graphite flakes without any binder we can also called it as free standing graphite sheet. During the process of exfoliation, an intercalated graphite flake expands typically by over 100 times along the *c*-axis. Compression of the resulting exfoliated graphite sheets causes to be mechanically interlocked to one another, so that the formed sheet will be without any binder.

Because of the exfoliation, flexible graphite has a large specific surface area (e.g. 15 m^2 g^{-1}). Due to the absence of a binder, flexible graphite is essentially entirely graphite. Hence as a result, flexible graphite is low in the coefficient of thermal expansion and is chemically and thermally resistant material. Due to its microstructure morphology involving graphite layers that are parallel to the surface of the sheet, flexible graphite is having high electrical and thermal conductivities in the plane of the sheet. Due to the connection in perpendicular direction of the graphite layers flexible graphite is electrically and thermally conductive in the perpendicular direction of the sheet. These in-plane and out-of-plane microstructures result in flexibility, which is very important for EMI gaskets. As it is having high electrical conductivity (especially that in the plane of the sheet) and high specific surface area in flexible graphite, the shieldingeffectiveness of this material for shielding is exceptionally high (up to 130 dB at 1 GHz)[10,21,23,25,28,47–49]

2.4. COLLOIDAL GRAPHITE

Colloidal graphite is a fine graphite powder which are suspended in a solvent (such as water and alcohol), along with a small amount of a polymeric binder material. After application of colloidal graphite on a surface by means of painting or any other methods, the solvent will evaporate, and thus allowing the graphite particles to be essentially in direct contact. Which results in the effective applications for EMI shielding. Which is commonly used for shielding in television scopes[8].

CHAPTER 3

3.0 EXPERIMENTAL TECHNIQUES

3.1MATERIALS REQUIRED:

Following materials has been used for the synthesis of GO

Graphite powder (CDH, India),sulfuric acid 98% (Merck),sodium nitrate (Fischer scientific)Potassium permanganate (Fischer scientific),hydrogen peroxide 30% solution(Specpure,India) hydrazine hydrate (Sigma Aldrich) and Double disitilled water was used for synthesis and washing.

3.2SYNTHESIS OF GRAPHITIC OXIDE (GO)

To prepare GO using Hummers Method we took a clean dry beaker and rinsed it using concentrated sulphuric acid. Then we added 75ml of $H_2SO_4$and stirred on magnetic stirrer and then added 3gm of $NaNO_3$.Stirred this solution for 1 hour, then added 3gm of graphite and stirred for 3 hours. Then added 9gm of $KMnO_4$ very slowly while keeping it on an ice bath and making sure that the temperature of the solution does not rise above 20 ℃. Stirred this solution on a magnetic stirrer for 24 hours. Then added 150 ml of water to this solution and stirred for 20 min and then added 420ml of water and stirred for 10 min. Then we added H_2O_2 to the solution till a bright yellow color is obtained. Then filtered the solution and washed the precipitate with water 2-3 times or till all the acid is removed. Centrifuged the solution and the GO pulp is removed.Fig. 3 shows a flow diagram of preaparation of graphitic oxide.

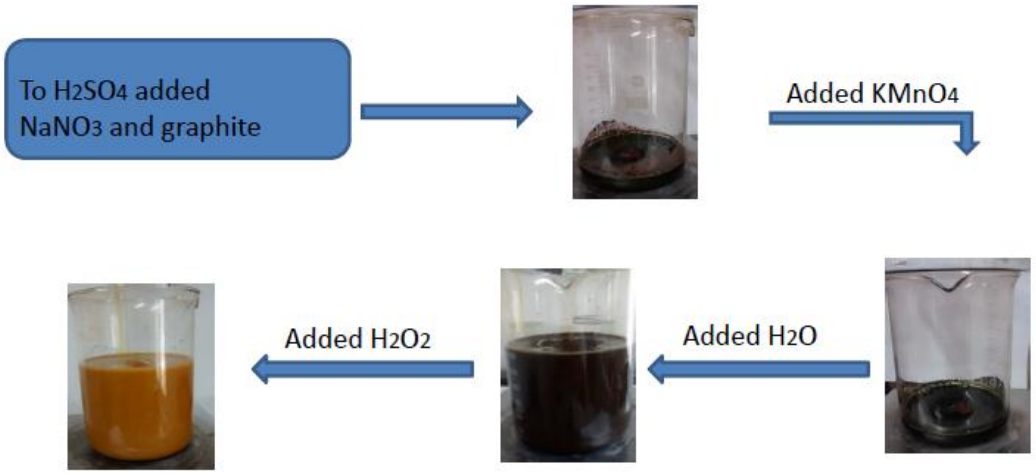

Fig.3. Flow diagram for the preparation of GO

During oxidation (shows in Fig.4)of grahpite oxygen functionalites group and epoxide group introduced to C atom and the interlayer spacing increases, because of this conjugation of the network damaged and epoxide group restricts the electron movement, hence increasing in the resistance.

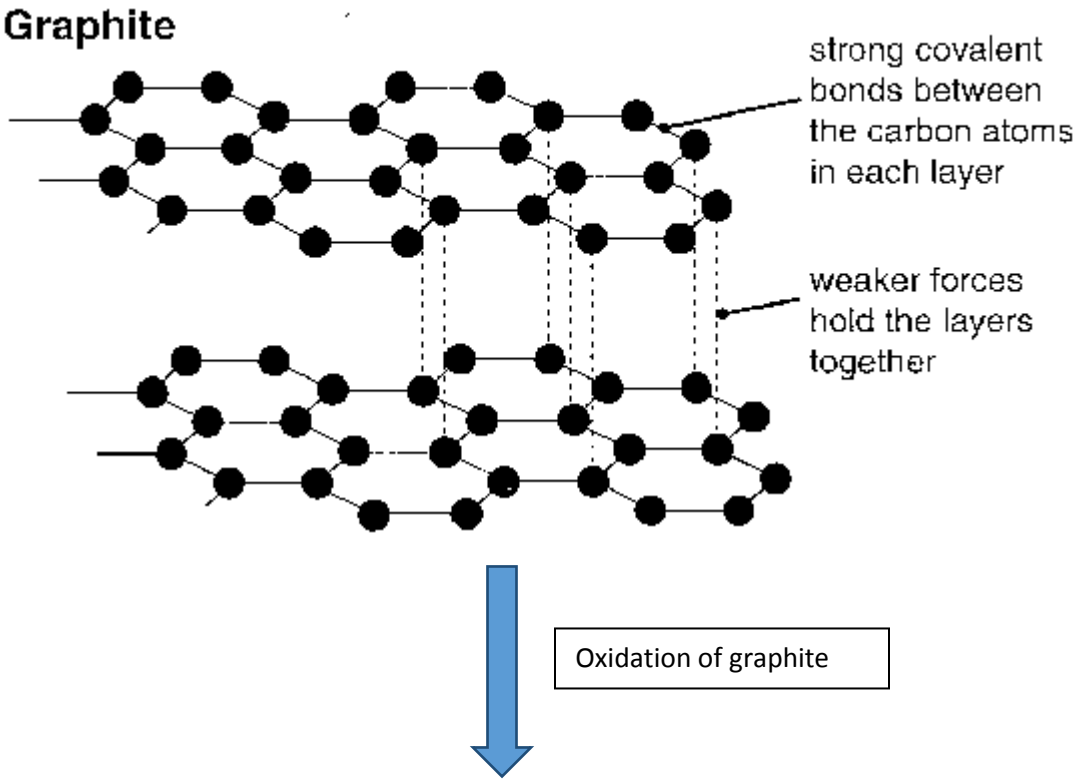

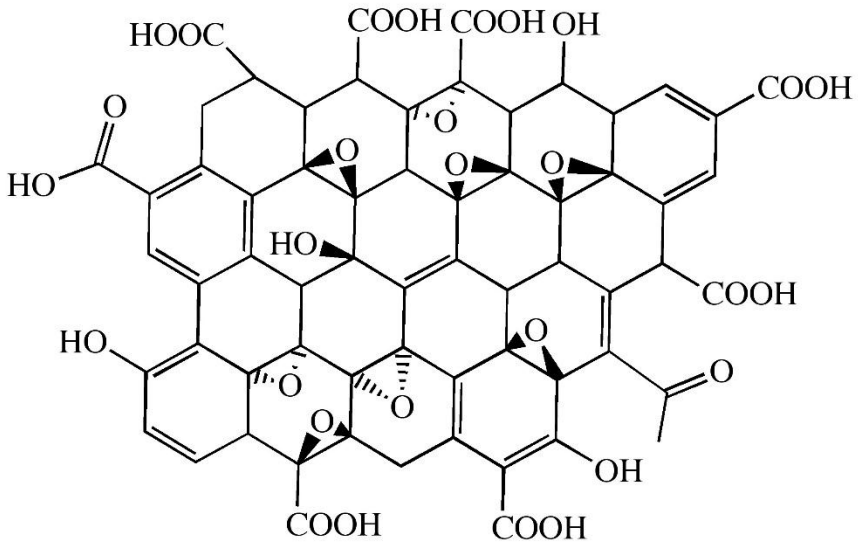

Fig.4 Flow diagram of oxidation of graphite

3.3 FABRICATION OF GRAPHITIC OXIDE PAPER

GO flakes by taking 3mg/ml concentration that has been prepared by hummer's method was dispersed in distilled water by ultrasonication process and followed by solvent casting over the acrylic pertidish. The sample has been kept at 35^0C for 24 hours to evaporate the water which gives a free standing GO paper of ~250 micron thickness and resistivity ~10^6 ohm/square. Prepared GOP hhas been shown in the Fig.5

Fig.5. Free standing GO paper

3.4 REDUCTION OF GRAPHITE AND FABRICATION OF CHEMICALLY REDUCED GRAPHITIC OXIDE PAPER

Reduction of graphitic oxide removes the oxygen functionalities group by means of chemically or thermally. In chemical reduction of graphitic oxide it uses Hydrazine and in thermal reduction reduction occurs by heating the graphitic oxide at a very high temperature.After reduction the conjugation restores and because of removal of oxygen functionalities group the interlayer spacing decreases and hence the conductivity increases. A typical chemical reduction process shown in the below Fig 6.

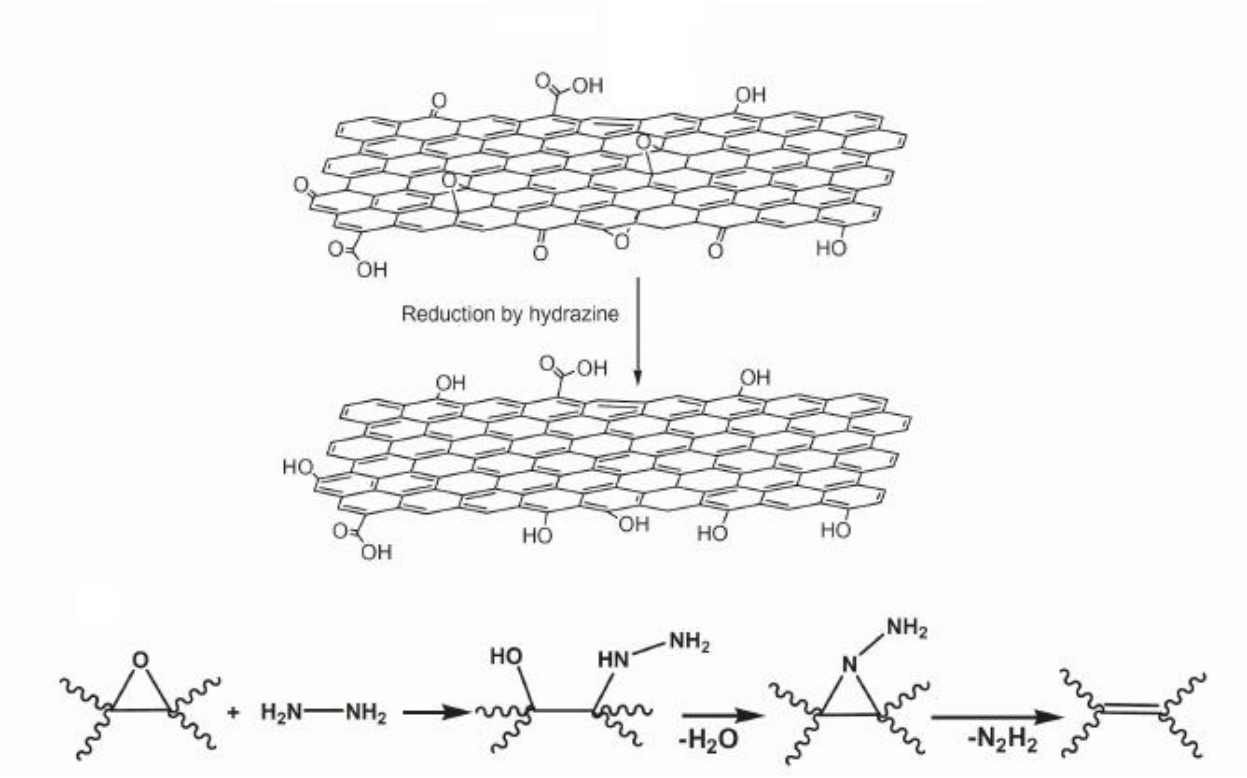

Fig 6. Reduction of graphitic oxide.

The prepared GO paper was kept in the hydrazine vapors for 12h in a closed chamber containing a solution of hydrazine. As hydrazine is a strong reducing agent it reduces the GO paper which

can be observe by The color of the GO paper in fig.7,which turned to black in colour from brown colour.

During the reduction of the paper there is an expansion or the distance between the stacks slightly increases which cause to increase in the thickness. Hence The resulted chemically reduced graphitic oxide paper had a thickness of 200 micron. Reduced GO paper is shown in the below Fig 7.

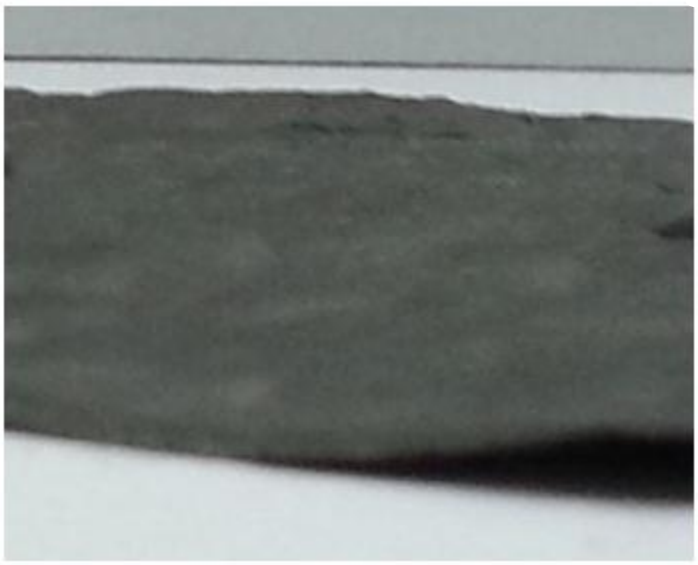

Fig.7. Reduced GO paper

3.5 CHARACTERIZATION AND MEASURMENTS:

The following characterization techniques has been used in our experiment.

1.XRD- The XRD patterns of GO paper and RGO paper were recorded by using Bruker D8 Advance X-ray diffractometer in the diffraction (2θ) range of 10-80^{o}, at a scan rate of 0.02^{0}/sec, slit width of 0.1 mm using CuKα line (λ= 1.540598Å) as radiation source.

2.FTIR- The Fourier transform infrared (FTIR) spectra of GO and RGO papers was recorded in the wave number range 400-4000 cm^{-1} (at a resolution of 4cm^{-1} and averaged over 32 scans) using diamond attenuated total reflectance (ATR) assembly attached to FTIR spectrometer (Agilent Technologies, Carry 630).

3.RAMAN-Raman microscope (Renishaw In Via) was used for recording Raman spectrum of samples in 1000 cm^{-1} - 3000 cm^{-1} wavenumber range with 514.5 nm laser as excitation source.

4.INDENTATION TEST-Hardness test of the sample is done by using the Nanoindenter instrument IBIS.

5.SHIELDING EFFECTIVENESS (SE)-shielding effectiveness was measured using a homemade free space measurement system containing a DC source powered 101 GHz microwave source-antenna couple and a horn-powermeter assembly based detector.

6.TENSILE TEST- Mechanical property of the paper was tested by using Universal Testing Machine INSTRON.

CHAPTER 4

4.0 RESULTS AND DISCUSSION:

4.1. XRD (X-ray diffraction) is an analytical tool used for the identification of atomic and molecular structure of crystals, in which the incident ray gets diffracted into many directions. By observing the intensities and the angles of the diffracted beam we can give a 3-Dimension picture of the electron density in the crystal and hence by using this information we can determine the various chemical bonds, disorder in the crystal and many other information like plane of the crystal, interlayer distance between the planes. In our present work we have done the XRD of the synthesized GOP and CRGOP, and a comparison is done with the pristine graphite. XRD spectra is measured in the range of 2Θ from 10° to 50°, which show a diffraction peak of pristine graphite at an angle of 26° and d which is distance between the layers is calculated by using Brags equation i.e.

$$2d \sin\Theta = n\lambda, \text{ ---------- (4)}$$

Which is nearly equal to 3.34Å, which is shown in the Fig.8.

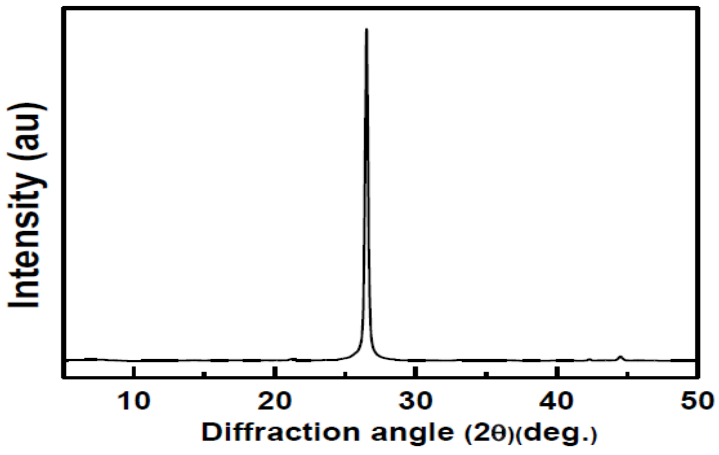

Fig.8 XRD spectra of graphite

As the oxygen functionalities group introduced to the graphite there is an expansion of the graphite layers and the interlayer spacing increases in the graphite, and hence the diffraction angle should be less. It is clearly observed in the XRD spectra of GO the diffraction angle of GOP is at an angle of 12° and hence the interlayer spacing of the stacks is nearly equal to 7.97 Å, and it is clearly

Visualize in Fig.9

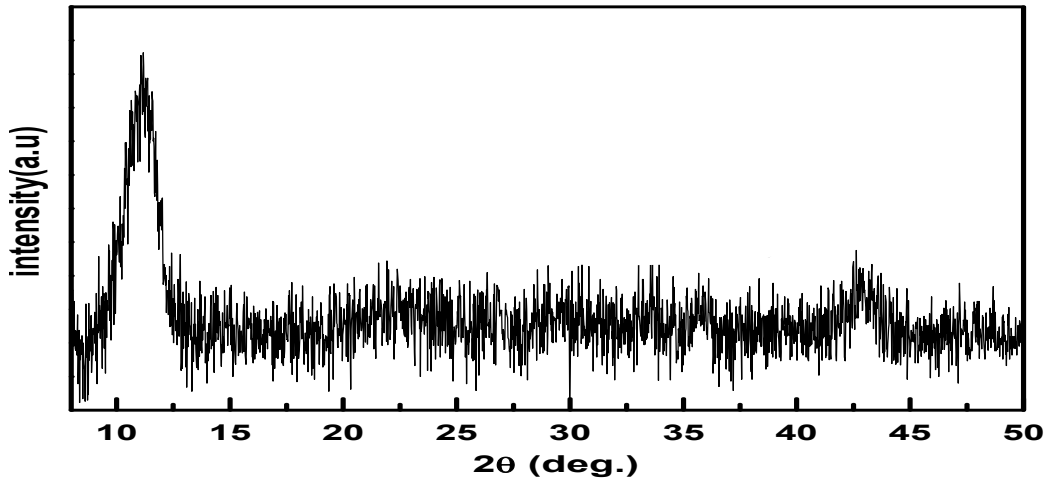

Fig.9 XRD spectra of graphitic Oxide

During the reduction of GO it is the process of removing the oxygen functionalities from the synthesized GO and hence cause the restacking of the sheets and hence decreases in the interlayer spacing of the sheets and shifting in the angle to the higher side. The spectra of rGO shows two peak one is near to 2Θ=12° which is due to the disordered components during the chemical synthesis of GO, and the other peak at an angle of 2Θ= 24.9° and d nearly equals to 3.57Å gives the information of successful reduction of GO to rGO, which is shown in Fig 10.

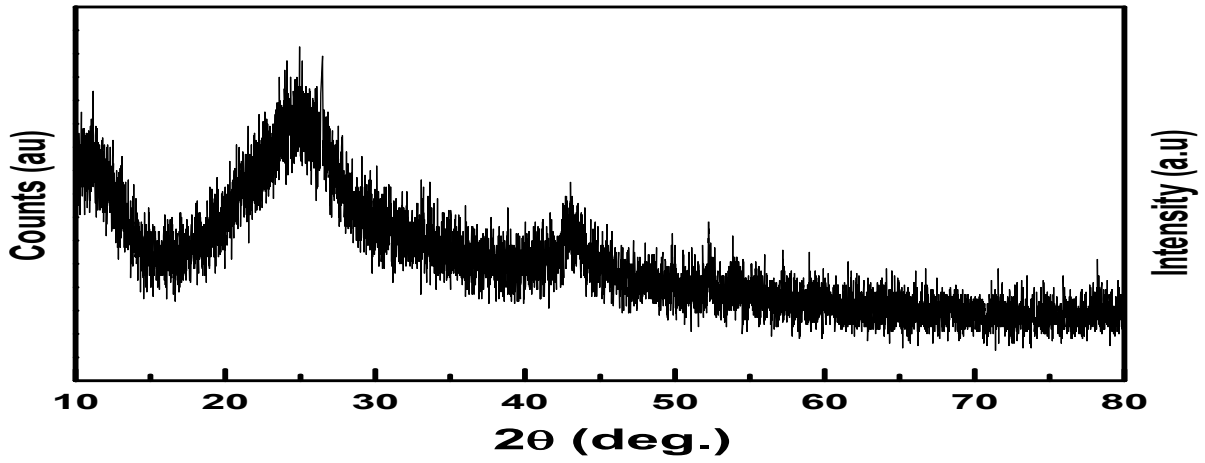

Fig.10 XRD spectra of reduced graphitic oxide

4.2. FTIR(FOURIER TRANSFORM INFRA RED) is a technique used to obtain the infrared spectrum of emission or absorption of a solid, liquid or gas. Absorption spectrum is used to measure how well a sample absorbs the light at which wavelength, by using this we can also find out, which functional group is attached at their vibrational frequency. ATR-FTIR spectrum of GO is shown in the given Fig. 11.

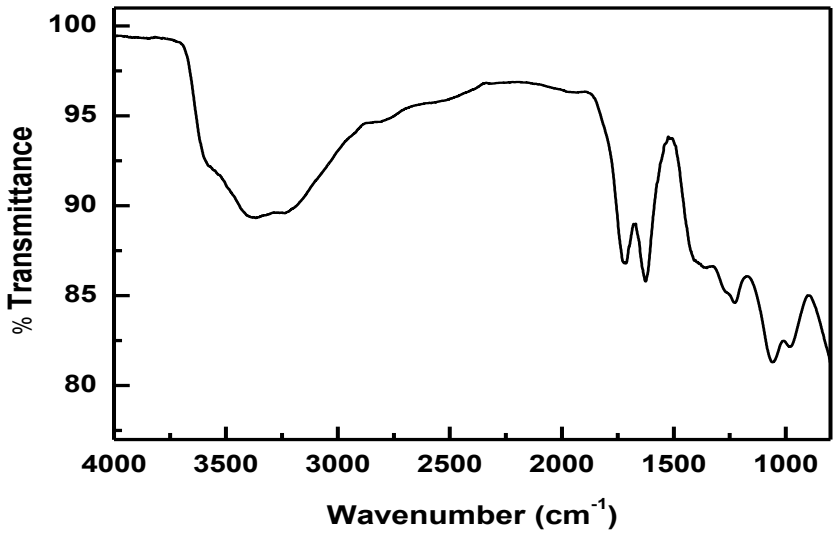

Fig.11. ATR-FTIR spectrum of Graphitic Oxide

A prominent adsorption peak appeared at 3396 cm^{-1}which revels the GO characteristics. This strong peak assigns to the stretching vibrations of the hydroxyl (O-H) and water. This O-H bond may be due to the presence of alcoholic, phenolic, carboxylic and so on. Because of presence of water at this vibrational frequency it also confirms the hydrophilic properties of prepared GO. Further peak at 1708 $cm^{-1}$and 1225cm^{-1}gives the stretching vibrations of carbonyl group (C=O) and the epoxide groups. The C=C stretch is present at the band of 1620cm^{-1}which gives the signature of unoxidised carbon groups. With regard the presence of different oxygen containing functional groups it can be verified that synthesized GO is highly hydrophilic in nature.

4.3. RAMAN-RAMAN SPECTROSCOPY is a very important tool suited for the molecular morphology characterization of the carbon materials, it is capable of characterize sharp or even slight changes in structure occurs. Raman spectrum is directly corresponds to the specific vibrational frequency of a bond within the molecule. The vibrational frequency and the position of the RAMAN band is very sensitive to the orientation of the band. In our experiment after preparation of GO we compare the RAMAN spectra of prepared GO and graphite. RAMAN spectra of graphite shows in Fig.12. The prominent peak of G (graphite) band because of sp^2 carbon at 1599$cm^{-1}$with negligible peak of D (defect) band. Raman spectra of graphite also confirms that the small ratio of I_D/I_G gives the ordered structure in terms of defects.

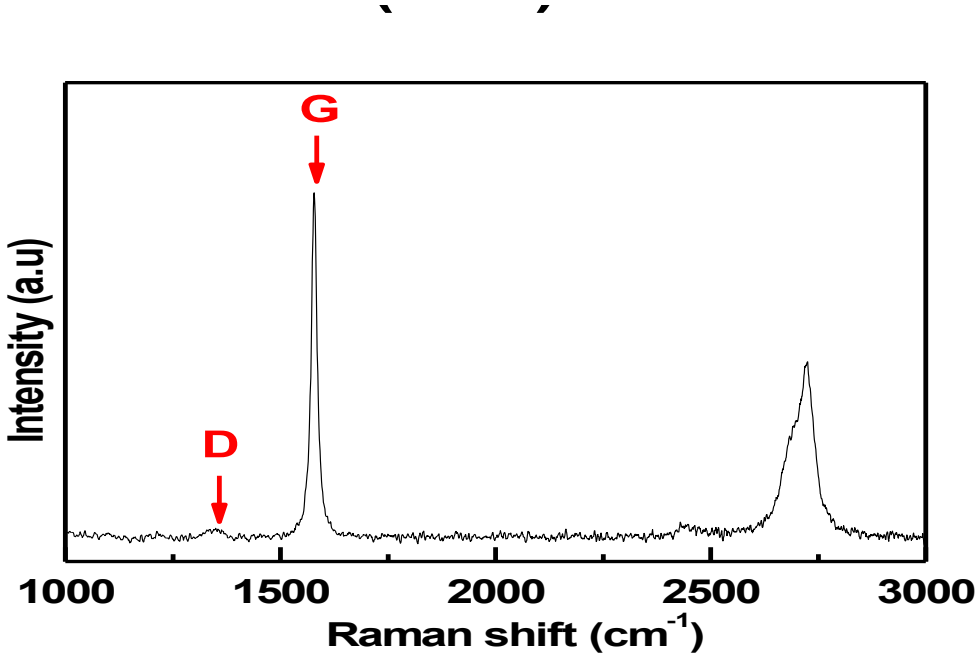

Fig.12 RAMAN spectra of graphite

After oxidation of graphite there is an introduction of oxygen functionalities group and the hybridization of carbon atom changes to sp^3 carbon atom, and formation of defect band occurs. the two dominating peak dominating peak of D band near to 1359 $cm^{-1}$and G band near to

1599cm[1],which clearly justify the oxidation of graphite and preparation of GO. Which is clearly shown in Fig.13.The increase value in the ratio of the intensity of D-band and G-band i.e. I_D/I_G also justify the oxidation of graphite and changes in the hybridization of carbon atom to sp^3

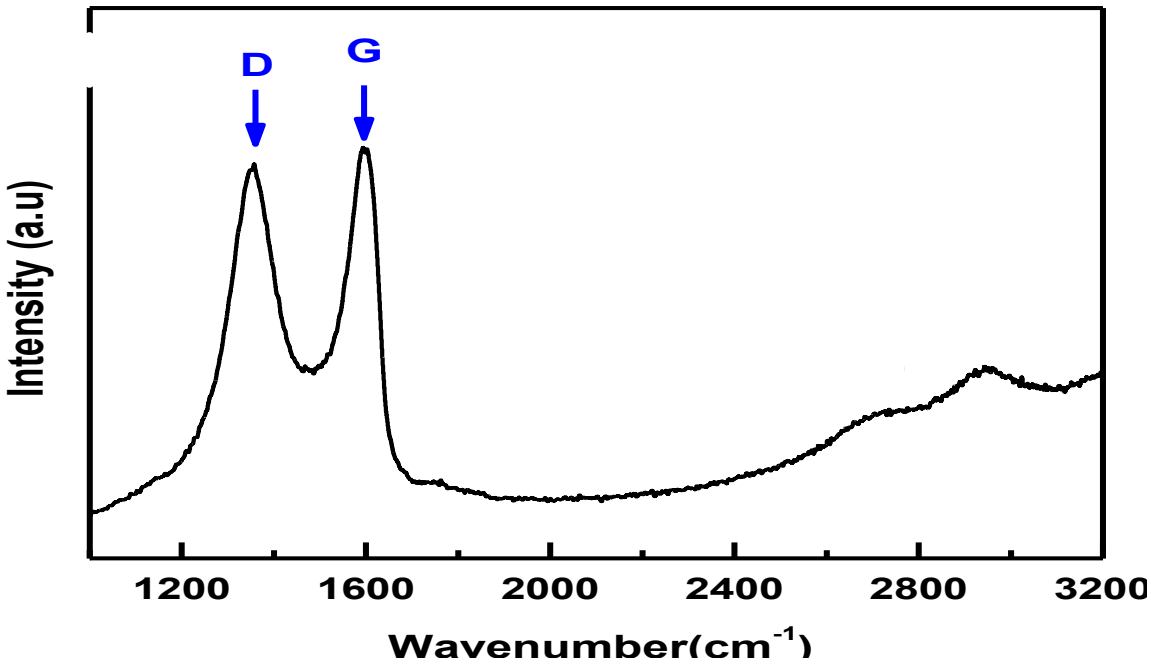

Fig.13. RAMAN spectra of graphitic oxide.

When we chemically reduced the GO in vapour phase of hydrazine we observe that there is a shift in the D band when we compare with the spectra of GO. Which is shown in Fig.14.

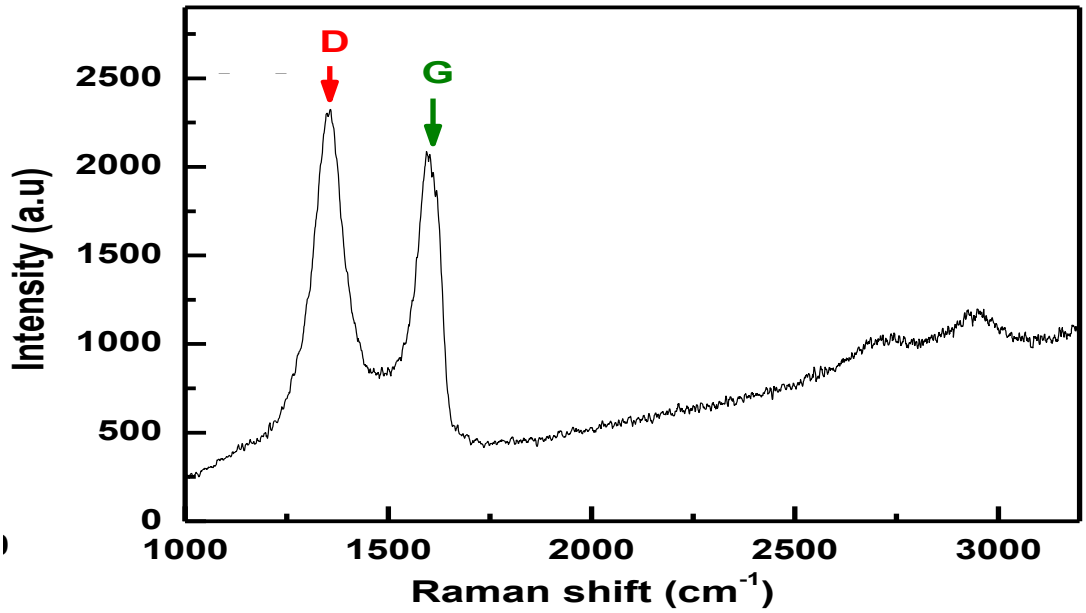

Fig.14. RAMAN spectra of reduced graphitic oxide.

The shifting in the band is due to the removal of oxygen functionalities group and the restacking of the sheets of the graphite layer occurs. Which also changes the hybridization state of carbon atom from $sp^3$to sp^2which is the justification of the reduced GO.

4.4. INDENTATION TEST –Indentation test is carried out by using Nano indentation instrument IBIS, which is used for the testing of mechanical properties of the materials. In a Nano indentation test small loads and tip sizes are used, so the indentation area may only be a few square micrometers or even nanometers. Whose mechanical properties are known is pressed into a sample whose properties are unknown. The load placed on the indenter tip is increased as the tip penetrates further into the sample having unknown mechanical property and soon reaches a user-defined value. At this point, the load may be held constant for a period or removed. A schematic Fig 15.of Nano indenter instrument and graph of load displacement curve for a Nano indentation test is as shown in the below Fig 16.

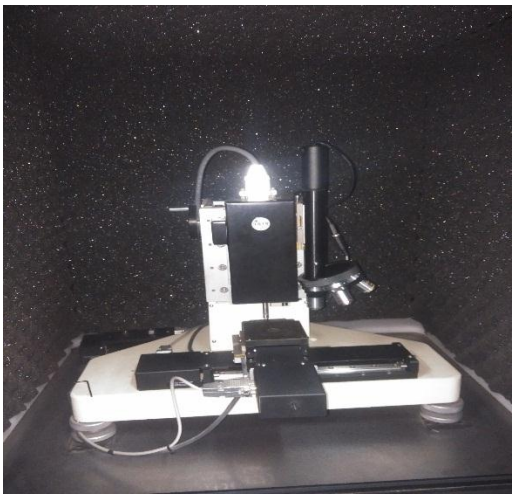

Fig.15 Nano indenter instrument IBIS

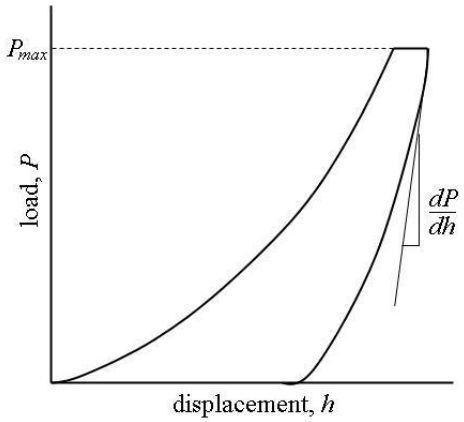

Fig.16 Load displacement curve

Where slope $\frac{dp}{dh}$ of the curve during unloading curve, is defined as the stiffness S of the contact.

The stiffness of the contact can be used to calculate the reduced Young's modulus E_r

$$E_r = \frac{1}{\beta}\frac{\sqrt{\pi}}{2}\frac{s}{\sqrt{A_p}}$$---------- (5)

Where A_p in equation 5 is the projected area of the indentation at the contact depth h_c, β is the geometrcical constant which is 1.167.

h_c is the contact depth and it is calculated by using the given equation no.6

$$h_c = h_{max} - \varepsilon\frac{P_{max}}{S}$$----------(6)

Where P_{max} is the maximum load applied to the test speciment, h_{max} is the maximum displacement after one cycle.The Hardness H of the material is defined as the ratio of maximum load applied to the material to the projected area and it is calculated by using the given equation no.7.

$$H = \frac{P_{max}}{A_p}$$----------(7)

A_p, is the area of projection and it depends on the sape of the indenter material, it is equal to $24.5h_c^2$.

Young's modulus of the test specimen is related to the reduced young's modulus by using the given equation no.8.

$$\frac{1}{E_r} = \frac{1-v_i^2}{E_i} + \frac{1-v_s^2}{E_s}$$----------(8)

Where $E_{r,}$ is the reduced young's modulus and v_i, $E_i$is the poisson's ratio and youngs modulus of the indenter material.

v_s,E_s is poissons ratio and young's modulus of the test sample.

This test is done by using IBIS instrumentsThe nanoindentation studies were performed by using the IBIS nanoindentation system (model B, Fisher Cripps Laboratories Pvt. Ltd, Australia). The maximum applicable load was 500 mN, with a force resolution of 500 nN, a depth of 20 µm and depth resolution of 0.03 nm. The face angle of the Berkovich indenter was 65.27^o and the tip radius was 100 nm., and the result is calculated as follows:

E_i, v_i is the young's modulus and poission's ratio of the of the diamond material,which is equal to 1140 Gpa and 0.07.

v_s is the poission's ratio of the sample, which is equal to .149[47].

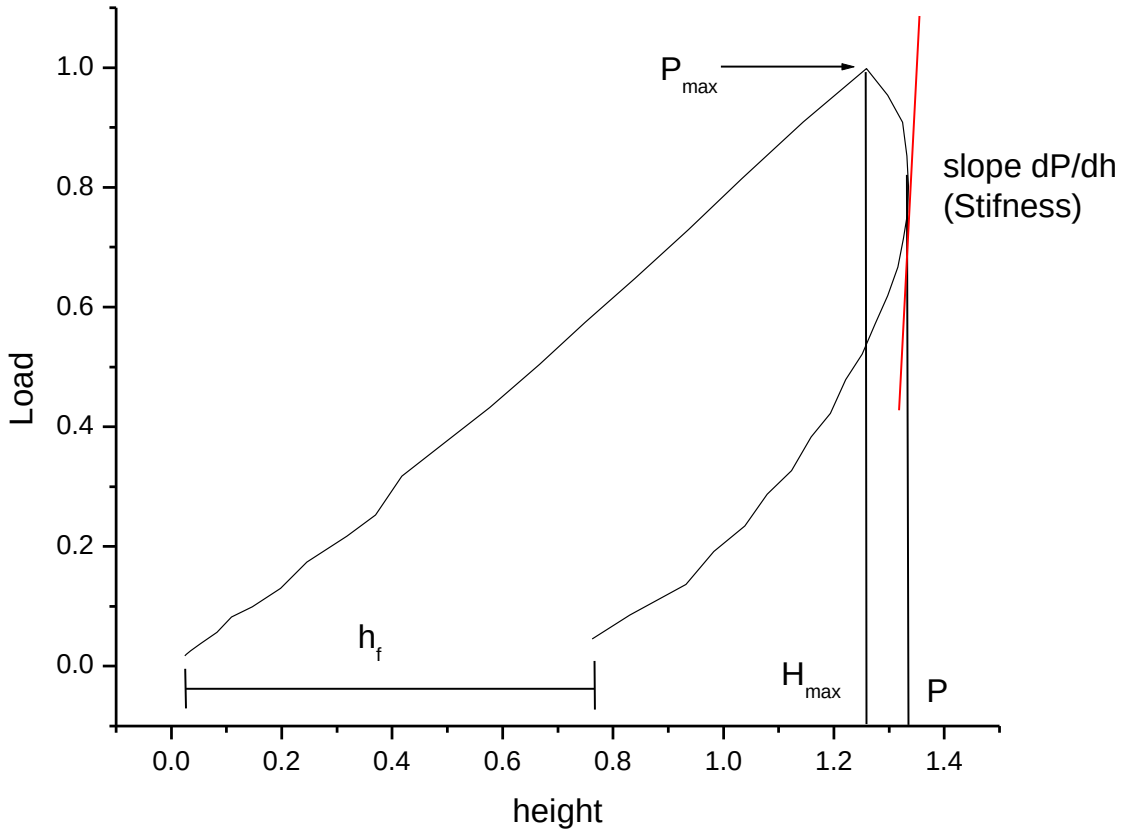

Fig.17 Load displacement curve of specimen

S= -5521.93 N/m, $h_c = 1.202 * 10^{-6}$ m, $A_p = 35.43*10^{-12}m^2$, H=$25.75 * 10^6$ N/m^2,$E_r = 704.49 * 10^6 N/m^2$, $E_s = 734.02 * 10^6$ N/m^2.

Percentage recovery of the material is calculated by using

$$\frac{H_{max}-h_f}{H_{max}} * 100 \quad \text{----------(9)}$$

where $h_f$is the final displacement after one cycle.Hence percentage recovery of the material is equal to 39.16%.

4.5. SHIELDING EFFECTIVNESS – The ratio of electric field magnitude or magnetic field magnitude without the shield material to with the shield material at a given distance from the source is defined as the shielding effectiveness. Shielding effectiveness (SE) that can be mathematically expressed by logarithmic ratio of strength of incident and transmitted power (Electric or magnetic field) which is shown in fig. 10.

$$SE\,(dB) = 10\log_{10}\left(\frac{P_T}{P_I}\right) = 20\log_{10}\left(\frac{E_T}{E_I}\right) = 20\log_{10}\left(\frac{H_T}{H_I}\right) \text{ ---------- (10)}$$

Where P_I(E_I or H_I) and P_T (E_T or H_T) are the power (electric or magnetic field intensity) of incident and transmitted electromagnetic waves respectively. As the ratio P_T/P_I (E_T/E_I or H_T/H_I) is always less than unity therefore from the equation, SE (total shielding effectiveness) is a negative quantitysuch that a shift towards more negative value means increase in magnitude of SE.

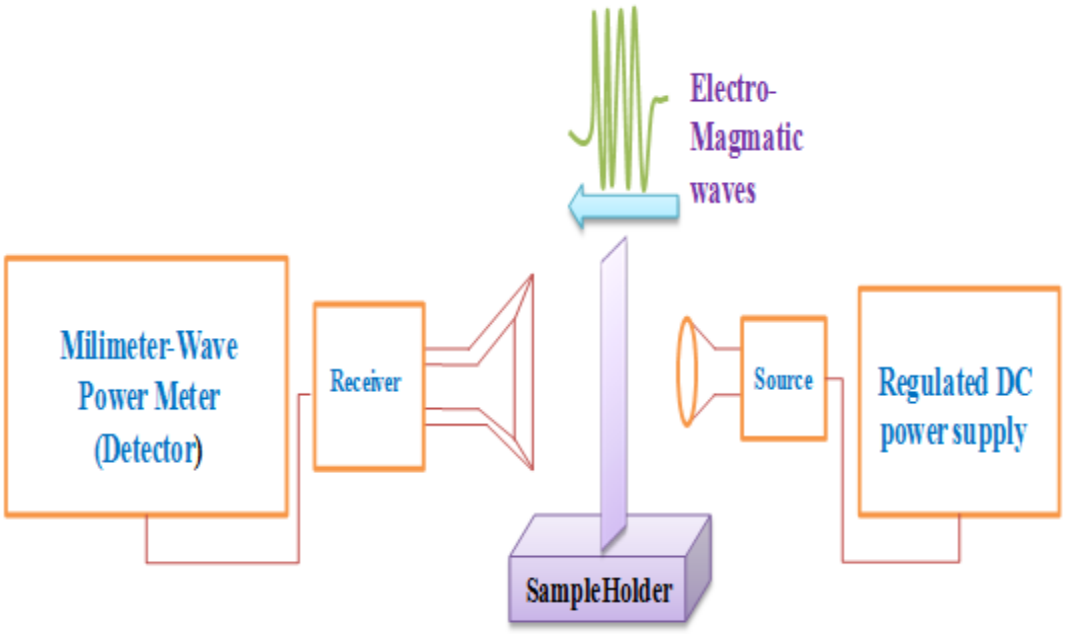

Fig. 18: Schematic of EMI shielding measurement setup

Fig. 18 shows the schematic of the EMI shielding measurement setup which consists of a regulated DC power supply to give input to a 101 GHz frequency microwave source coupled to a circular horn type antenna. The antenna generates a beam of microwave energy which is propelled through free space to reach a rectangular type antenna which is connected to a detector (i.e. millimeter wave power meter). The measurements are completed by alternatively measuring the power reaching the detector in the absence and presence of the sample to assess corresponding incident power (P_I) and transmitted power (P_T) respectively. The calculated SE value for (graphitic oxide paper) GOP, (chemically reduced graphitic oxide paper) CRGOP and (extended graphitic sheet) EGS samples is reported in the Table 3.

Material	**Input power (mW) P_i**	**Transmitted power(nW)P_t**	**Shielding Effectiveness(SE) (dB)**	**Percentage blocking (%)**	**Specific SE (SSE) (db.cm^3/g)**
GOP	.296	$2.07x10^5$	-1.55	30	-1.61
CRGOP	.298	84.2	-35.49	99.97	-221.8
EGS	.296	81.3	-35.61	99.97	-34.57

Table 3. EMI shielding effectiveness (SE) and specific SE values for samples

It can be seen that the GO paper gives negligible attenuation (only 30% radiation blocking) with SEvalue of only -1.55 dB . The low SE value of GOP may be linked to the poor conductivity and related conduction loses, due to loss of conjugation via oxidation induced sp^3 defects (oxygen functionalities). In contrast, the CRGOP shows very high attenuation with SEvalue of -35.49 dB, which represent its capability of blocking more than 99.97 % of the incident EM energy. Such high SE of can be ascribed to the high electrical conductivity owing to restoration of conjugation upon reduction process. In order to compare the attenuation characteristics of

CRGOP with other carbon analogues, SE of expanded graphite sheet (EGS) is also measured and reported in Table.. Interestingly, it is observed that despite its very high conductivity (120 S/cm); EGS display similar attenuation levels as CRGOP. This suggests that EMI shielding mechanisms of EGS and CRGOP are different and further studies in the direction are necessary to unveil the same. Nevertheless, in order to demonstrate the superiority of CRGOP, SSE values (SE per unit density) were calculated and it was observed that SSE value of CRGOP (~ -221.8 $dB.cm^3/g$) is much higher compared to EGS (~ -34.57 $dB.cm^3/g$). Indeed, this value is significantly higher than low SSE value of copper sheet ~ -10 $dB.cm^3/g$.

4.6.TENSILE TEST – GOP were tested by dynamic mechanical analyzer (INSTRON machine) under uniaxial in-plane tension with 2 mm/mindisplacement rate. GOP under uniform axial loading are states of plane stress in one dimension. A schemetic figure. of test result of INSTRON machine is shown in Fig.19

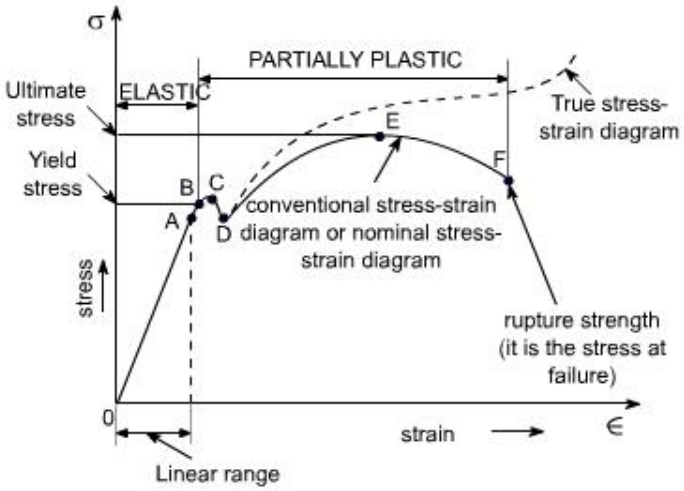

Fig19. Stress Strain curve generated by UTM

The INSTRON machine used for the testing the specimen determines stretch and tensile force of GOP in time-steps and provides stress and strain amounts based on their dimensions and following equations.

$$\varepsilon_x = u_x \text{----------(11)}$$

Where, $\varepsilon_x = u_x$ is the strain and displacement in X direction.

$$\sigma_x = \frac{F}{A} \text{----------(12)}$$

Where, σ_x, F, A is the stress in the X- direction, tensile force and cross section area of the specimen.

$$\varepsilon_x = \frac{1}{E}(\sigma_x - v\sigma_y)\text{----------(13)}$$

Where, $v, \sigma_y$is the poisson's ratio of the specimen and stress in the Y direction, and E is the young's modulus.

Fig. 20 demonstrates the stress-strain curve of GOP. These curve shows roughly linear behaviour which demonstrates the elastic behaviour of the material.

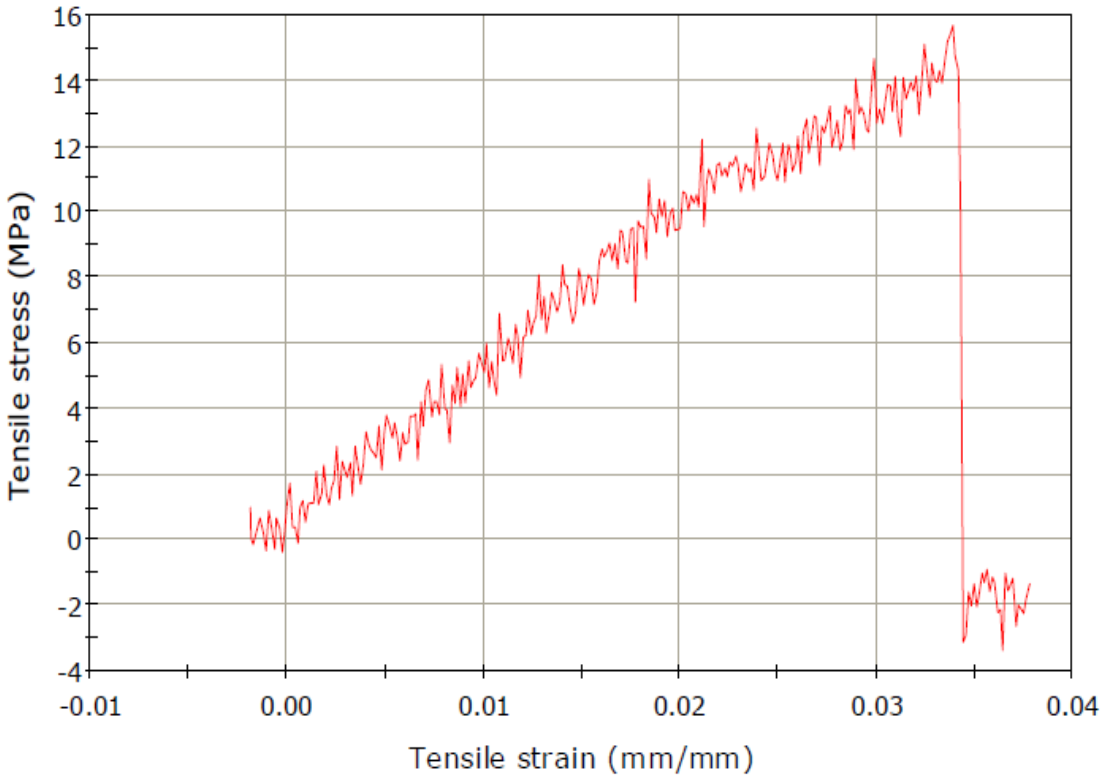

Fig.20 stress-strain curve of GOP

From the above graph we can calculate Stiffness (s) it is an extensive material property, which can be defined as a resistance of elastic body to stretch (δ).

$$s = \frac{F}{\delta} \text{----------(14)}$$

Relationship between Young's modulus and stiffness is determined as below,

$$S = \frac{AE}{L} \text{---------- (15)}$$

Where, L is the length of the specimen, E is the young's modulus and A is the area of the sample.

Dimensions and results of specimen is shown in the given Fig.21, the ultimate tensile strength of our specimen it can be seen from the graph clearly it is almost 15Mpa.

Young's modulus of the GO paper is 518.66790 MPa, and stiffness and elongation has been calculated from the above equation and is found as 518.66790 N/m and $7.55*10^{-6}m$.

.

Results Table 1

	Maximum Load (kN)	Tensile extension at Maximum Load (mm)	Tensile stress at Maximum Load (MPa)	Length (mm)
1	0.00392	0.84813	-1.30816	25.00000

	Thickness (mm)	Width (mm)	Area (mm^2)	Extension at Break (Standard) (mm)
1	0.02500	10.00000	0.25000	0.99078

	Tensile strain at Break (Standard) (mm/mm)	Maximum Extension (mm)	Load at Maximum Extension (N)	Modulus (Automatic) (MPa)
1	0.03781	0.99078	-0.32704	518.66790

	Modulus (Automatic) (MPa)	Final area (cm^2)
1	518.66790	0.03600

Fig.21 Data of Specimen Sample by UTM

CHAPTER 5

CONCLUSION:

The chemically reduced GO paper has been successfully synthesised by solution casting of chemically derived GO, subsequent drying and final reduction using hydrazine hydrate. The formed reduced GO based paper (CRGOP) is charecterised using different techniques including FTIR & Raman spectroscopy and X-ray diffraction, which confirm the phase formation and successful oxidation of graphite to GO and its subsequent reduction to RGO. The formed RGO paper is found to flexible, mechnicall strong and electrically conducting.The nanoindentation test gives the indentation hardness value of 5521.93 N/m and elastic modulus value of $734.02x10^6$ N/m^2. The tensile testing shows the tensile strength and modulus value of 15 MPa and 518.66790 MPa respectively. The EMI shielding effectivness value of the RGO paper was found to be -35.49 dB, which was significantly higher compared to the GO paper (only -1.55 dB). This RGO paper with moderate stifness , good flexibility, high tensile strength and high specific shielding effectiveness value, can be used an EMI shiled gasketing material.

FUTURE SCOPE:

In the present work, synthesized RGO paper has been successfully demonstrated for good EMI shielding response. However, due to promising properties of graphene, it is also expected to be useful for other applications, by regulation & tuning of microstructure, conductivity, surface chemistry and mechanical properties of the material/product. The graphene paper may be chemically or thermally treated to improve the contributions of multiple reflection & absorption, at the same time reducing reflection. The thin strip of material, with combination of porosity & electrical conductivity, may also be explored as electrode material for supercapacitor. The control of permeability and wet strength may also allow the use in water purification applications.

REFERENCES:

1. Saini, P. in *Fundamentals of Conjugated Polymer Blends, Copolymers and Composites* (ed. Saini, P.) 449–518 (John Wiley & Sons, Inc., 2015).
2. Saini, P. in *Thermoset Nanocomposites* (ed. Mittal, V.) 211–237 (Wiley-VCH Verlag GmbH & Co. KGaA, 2013).
3. Yang, Y., Gupta, M. C., Dudley, K. L. & Lawrence, R. W. Novel carbon nanotube-polystyrene foam composites for electromagnetic interference shielding. *Nano Lett.* **5,** 2131–2134 (2005).
4. Li, T.-T., Wang, R., Lou, C.-W., Lin, M.-C. & Lin, J.-H. Manufacture and effectiveness evaluations of high-modulus electromagnetic interference shielding/puncture resisting composites. *Text. Res. J.* **83,** 1796–1807 (2013).
5. Saini, P., Choudhary, V., Singh, B. P., Mathur, R. B. & Dhawan, S. K. Polyaniline–MWCNT nanocomposites for microwave absorption and EMI shielding. *Mater. Chem. Phys.* **113,** 919–926 (2009).
6. Saini, P. & Choudhary, V. Enhanced electromagnetic interference shielding effectiveness of polyaniline functionalized carbon nanotubes filled polystyrene composites. *J. Nanoparticle Res.* **15,** (2013).
7. Saini, P., Choudhary, V., Singh, B. P., Mathur, R. B. & Dhawan, S. K. Enhanced microwave absorption behavior of polyaniline-CNT/polystyrene blend in 12.4–18.0GHz range. *Synth. Met.* **161,** 1522–1526 (2011).
8. Saini, P. & Choudhary, V. Structural details, electrical properties, and electromagnetic interference shielding response of processable copolymers of aniline. *J. Mater. Sci.* **48,** 797–804 (2013).

9. Saini, P., Choudhary, V., Vijayan, N. & Kotnala, R. K. Improved Electromagnetic Interference Shielding Response of Poly(aniline)-Coated Fabrics Containing Dielectric and Magnetic Nanoparticles. *J. Phys. Chem. C* **116,** 13403–13412 (2012).
10. Saini, P. & Aror, M. in *New Polymers for Special Applications* (ed. De Souza Gomes, A.) (InTech, 2012).
11. Taka, T., Nyholm, P., Laakso, J., Loponen, M. T. & Österholm, J. E. Determination of impurity effects of solubility and processability of poly(3-octyl thiophene). *Synth. Met.* **41,** 899–902 (1991).
12. Saini, P. *Fundamentals of conjugated polymer blends, copolymers and composites: synthesis, properties and applications*. (2015).
13. Saini, P. & Arora, M. Formation mechanism, electronic properties & microwave shielding by nano-structured polyanilines prepared by template free route using surfactant dopants. *J. Mater. Chem. A* **1,** 8926 (2013).
14. Eswaraiah, V., Sankaranarayanan, V. & Ramaprabhu, S. Functionalized Graphene-PVDF Foam Composites for EMI Shielding. *Macromol. Mater. Eng.* **296,** 894–898 (2011).
15. Zhang, B. *et al.* Microwave absorption enhancement of Fe_3O_4 /polyaniline core/shell hybrid microspheres with controlled shell thickness. *J. Appl. Polym. Sci.* **130,** 1909–1916 (2013).
16. Fletcher, A., Gupta, M. C., Dudley, K. L. & Vedeler, E. Elastomer foam nanocomposites for electromagnetic dissipation and shielding applications. *Compos. Sci. Technol.* **70,** 953–958 (2010).

17. Verma, P., Saini, P. & Choudhary, V. Designing of carbon nanotube/polymer composites using melt recirculation approach: Effect of aspect ratio on mechanical, electrical and EMI shielding response. *Mater. Des.* **88,** 269–277 (2015).
18. Liang, J. *et al.* Electromagnetic interference shielding of graphene/epoxy composites. *Carbon* **47,** 922–925 (2009).
19. Verma, P., Saini, P., Malik, R. S. & Choudhary, V. Excellent electromagnetic interference shielding and mechanical properties of high loading carbon-nanotubes/polymer composites designed using melt recirculation equipped twin-screw extruder. *Carbon* **89,** 308–317 (2015).
20. Yu, F. *et al.* Anisotropic multilayer conductive networks in carbon nanotubes filled polyethylene/polypropylene blends obtained through high speed thin wall injection molding. *Polymer* **54,** 6425–6436 (2013).
21. Chung, D. D. . Electromagnetic interference shielding effectiveness of carbon materials. *Carbon* **39,** 279–285 (2001).
22. Li, N. *et al.* Electromagnetic interference (EMI) shielding of single-walled carbon nanotube epoxy composites. *Nano Lett.* **6,** 1141–1145 (2006).
23. Tripathi, S. N., Saini, P., Gupta, D. & Choudhary, V. Electrical and mechanical properties of PMMA/reduced graphene oxide nanocomposites prepared via in situ polymerization. *J. Mater. Sci.* **48,** 6223–6232 (2013).
24. Zhang, Y. *et al.* Broadband and Tunable High-Performance Microwave Absorption of an Ultralight and Highly Compressible Graphene Foam. *Adv. Mater.* **27,** 2049–2053 (2015).

25. Chen, Z., Xu, C., Ma, C., Ren, W. & Cheng, H.-M. Lightweight and Flexible Graphene Foam Composites for High-Performance Electromagnetic Interference Shielding. *Adv. Mater.* **25,** 1296–1300 (2013).
26. Zhang, H.-B., Yan, Q., Zheng, W.-G., He, Z. & Yu, Z.-Z. Tough Graphene−Polymer Microcellular Foams for Electromagnetic Interference Shielding. *ACS Appl. Mater. Interfaces* **3,** 918–924 (2011).
27. Singh, S. *et al.* A highly porous, light weight 3D sponge like graphene aerogel for electromagnetic interference shielding applications. *RSC Adv* **5,** 107083–107087 (2015).
28. Cao, M.-S., Wang, X.-X., Cao, W.-Q. & Yuan, J. Ultrathin graphene: electrical properties and highly efficient electromagnetic interference shielding. *J Mater Chem C* **3,** 6589–6599 (2015).
29. Jing, X., Wang, Y. & Zhang, B. Electrical conductivity and electromagnetic interference shielding of polyaniline/polyacrylate composite coatings. *J. Appl. Polym. Sci.* **98,** 2149–2156 (2005).
30. Geetha, S., Satheesh Kumar, K. K., Rao, C. R. K., Vijayan, M. & Trivedi, D. C. EMI shielding: Methods and materials-A review. *J. Appl. Polym. Sci.* **112,** 2073–2086 (2009).
31. B.S.Dasaradan, R. P. Optimization of electromagnetic shielding tester process parameters for conductive textile composite materials through Taguchi design and ANOVA. **40 (2011),** 5477–5482 (2011).
32. D.D.L Chung. Materials for Electromagnetic Interference Shielding. **9(3),** 351 (2000).
33. Lundgren, U., Ekman, J. & Delsing, J. Shielding Effectiveness Data on Commercial Thermoplastic Materials. *IEEE Trans. Electromagn. Compat.* **48,** 766–773 (2006).

34. Guan, H., Liu, S., Duan, Y. & Cheng, J. Cement based electromagnetic shielding and absorbing building materials. *Cem. Concr. Compos.* **28,** 468–474 (2006).
35. H.K.Lee, B. R. K. Experiments to Investigate Electromagnetic Shielding Performance of Polyaniline coated thin films. **1,** (2010).
36. Thomassin, J.-M. *et al.* Polymer/carbon based composites as electromagnetic interference (EMI) shielding materials. *Mater. Sci. Eng. R Rep.* **74,** 211–232 (2013).
37. D.D.L. Chung, X. L., D. D. L.Chung. Electromagnetic interference shielding using continuous carbon-fiber carbon-matrix and polymer-matrix composites. 227–231 (1999).
38. Gelves, G. A., Al-Saleh, M. H. & Sundararaj, U. Highly electrically conductive and high performance EMI shielding nanowire/polymer nanocomposites by miscible mixing and precipitation. *J Mater Chem* **21,** 829–836 (2011).
39. Wen, S. & Chung, D. D. . Electromagnetic interference shielding reaching 70 dB in steel fiber cement. *Cem. Concr. Res.* **34,** 329–332 (2004).
40. I. Iordache, C. M. Electrical conductivity and electromagnetic shielding effectiveness of silicone rubber filled eith ferrite and graphite powders. **21,** 93–104 (2011).
41. Jagatheesan, K., Ramasamy, A., Das, A. & Basu, A. Fabrics and their composites for electromagnetic shielding applications. *Text. Prog.* **47,** 87–161 (2015).
42. D Shivute1, C. von K. Metallic filler powders to improve electromagnetic shielding of FRP laminates.
43. Tzeng, S.-S. & Chang, F.-Y. EMI shielding effectiveness of metal-coated carbon fiber-reinforced ABS composites. *Mater. Sci. Eng. A* **302,** 258–267 (2001).
44. Jonathan McConnell, S. R. Electromagnetic Shielding Properties of Carbon Fibre Composites in Avionic Systems.

45. D.D.L Chung, X. S. submicron nickel filaments made by electroplating carbon filaments as a new filler material for electromagnetic interference shielding.
46. Nayak, L., Khastgir, D. & Chaki, T. K. A mechanistic study on electromagnetic shielding effectiveness of polysulfone/carbon nanofibers nanocomposites. *J. Mater. Sci.* **48,** 1492–1502 (2013).
47. Ranjbartoreh, A. R., Wang, B., Shen, X. & Wang, G. Advanced mechanical properties of graphene paper. *J. Appl. Phys.* **109,** 14306 (2011).
48. Azim, S. S., Satheesh, A., Ramu, K. K., Ramu, S. & Venkatachari, G. Studies on graphite based conductive paint coatings. *Prog. Org. Coat.* **55,** 1–4 (2006).
49. Modak, P., Kondawar, S. B. & Nandanwar, D. V. Synthesis and Characterization of Conducting Polyaniline/Graphene Nanocomposites for Electromagnetic Interference Shielding. *Procedia Mater. Sci.* **10,** 588–594 (2015).